Investigation of temporal coherence and related issues during the Littoral Continuous Active Sonar 2016 trial

Simon Lourey and James Lau

Maritime Division, Defence Science and Technology Group, Edinburgh, Australia

ABSTRACT

In traditional pulsed active sonar (PAS) systems, the projector transmits for a short interval and most of the operating cycle is spent listening for echoes. Continuous Active Sonar (CAS) transmits continuously and relies on the modulation of the transmission to distinguish the (weak) echoes from the (very strong) direct transmission. In theory, detection performance in the presence of noise and direct transmission interference is improved by increasing the integration period of the detector. In reality the useful integration period is limited to the period that the channel is (approximately) stationary or coherent. Exceeding the coherence length can result in reduced detection performance due to destructive interference in the detector. Channel coherence length is known to be time-variable and it is important to guard against the use of channel characterisations that are no longer valid. In this paper we explore these effects using data from the Littoral Continuous Active Sonar 2016 (LCAS' 16) trial, with a goal of understanding the relationship between coherence length and detection performance. Finally we explore how detection performance is affected by choice of integration length.

1 INTRODUCTION

Recently there has been interest in Continuous Active Sonar (CAS) as an alternative to Pulsed Active Sonar (PAS) as applied to active underwater acoustic detection using sonar. PAS, the usual approach, works by transmitting for a small fraction of the sonar operating cycle and then listening for echoes with the sonar projector off, before making another short transmission at the start of the next cycle. CAS transmits for most (or all) of the cycle, which introduces problems with the dynamic range of the signal level in the receiver, and interference with the echo detection process by the continuing transmission. These problems are fundamentally caused by the direct transmission contributing much more power to the received signal than the echoes from the target. Similar problems are also observed in full duplex wireless communications (Zhang, et al. 2016). Despite these issues, continuous transmission may offer advantages, such as avoiding missed detections due to brief fades in the acoustic channel, and the ability to exploit brief periods of enhanced echo strength when a manoeuvring target presents a geometry that produces specular sonar returns to the sonar system.

As an invited member of NATO's Multi National Joint Research Project (MN-JRP), the Defence Science and Technology Group, along with other international defence agencies, is exploring potential applications of CAS systems in a litoral environment. The work presented here reports on the analyses of the MN-JRP Littoral Continuous Active Sonar (LCAS) data gathering trial conducted in October 2016 (LCAS-16) in the Gulf of Toranto, Italy.

A fundamental issue in operating a CAS system is the integration period of the matched filter used to detect echoes. Typically a CAS system will transmit at lower power levels to improve the dynamic range and/or to conserve energy of a battery powered system. This implies that long integration periods must be used to mitigate the effect of noise and the interference from the (very strong) direct transmissions. The detector integration length is in practice limited by environmental properties of the acoustic channel. These environmental properties and their effect on sonar processing are the focus of this report and earlier papers by Plate and Grimmett (Plate and Grimmett 2015) (Plate and Grimmett 2016).

The improvement in detectability as the coherent detector integration length is increased depends on how coherent the received signal is during the integration period. Temporal coherence is lost because of fluctuations in the channel delay caused by random variation in the motion of the medium, projector, target and receiver. To

characterise the temporal coherence properties of the channel, a statistic known as the coherence time or coherence length is measured, which represents the time separation for the coherence to fall to a specified fraction of the ideal value. This parameter is inversely proportional to the spreading of the signal in frequency caused by the random motions described above. Coherence length has been measured in experiments (Yang 2006) and theories exist on causative frequency spreading as induced by internal waves (Yang 2010). A difficulty in underwater acoustics is that factors other than internal waves can spread the signal in frequency (platform motion, surface waves etc.) (van Walree 2013), and if they are predominant, the dependence of coherence length on frequency and range will be weaker (Yang 2010).

Another environmental effect that can impact detection performance is multipath propagation. This results in spreading of the signal in time. The dual relationship between time and frequency means that this temporal spreading limits the bandwidth over which the signal is coherent. It has been suggested that the special characteristics of the Linear Frequency Modulated (LFM) chirp mean that for this signal, temporal and frequency spreading are in a sense equivalent (Baggenstoss 1994). This is because a frequency shifted LFM pulse is very similar to a delayed LFM pulse.

One method to mitigate temporal coherence issues (caused by variation of the channel) is to reduce the length of the matched filter to be less than the coherence time of the channel. Similarly if multipath propagation limits the coherent bandwidth, the detection performance can be improved by reducing the bandwidth of the matched filter. In the LCAS-16 trial, CAS detection was attempted using LFM waveforms, so that reducing the integration time (while keeping sweep rate constant) also reduces the matched filter bandwidth . This implies that losses caused by the moving ocean and multipath propagation cannot be separately distinguished and the same mitigation strategy applies to both cases (in the special case of the LFM waveform).

This paper is organised as follows. In section 2, temporal and spectral coherence are defined, and the estimator that will be used to measure temporal coherence is presented. The dependence of temporal coherence on range and frequency is discussed, as well as the incoherent (or square law) detector used to detect signals that are not coherent over the full duration of the transmission. In section 3 results are presented. Sub-section 3.1 discusses measurement of coherence and phenomena that were observed in the measurements. Subsection 3.2 discusses a detection experiment and the impact that the selection of coherent processing time has on detection performance. In section 4, conclusions and future work are presented.

2 PRELIMINARIES

The temporal coherence of a signal is defined (Yang 2006) as

$$\rho(t,\tau) = \frac{\langle p^*(t)p(t+\tau)\rangle}{\sqrt{\langle p^*(t)p(t)\rangle\langle p^*(t+\tau)p(t+\tau)\rangle}} \tag{1}$$

where $p(t)$ is the received signal at time t. Temporal coherence is used as a measure of detection performance due to changes in the channel during the period τ. Equation 1 cannot be evaluated directly because of the use of ensemble averages (denoted by <>). Estimation of the coherence requires replacement of the ensemble averages with averages over time, space (an array) or frequency. A typical measure of temporal coherence is the coherence time ($\tau_{1/e}$) and is the delay that is required for the coherence to fall to $1/e$.

In this work coherence will be measured using signals that consist of a train of identical pulses. Then the coherence is estimated using

$$\hat{\rho}([n-m]T) = \frac{\max_{\xi}\left|\sum_{k=1}^{T_p} p(kT_s+mT)p^*(kT_s+nT+\xi)\right|}{\sqrt{\sum_{k=1}^{T_p}|p(kT_s+mT)|^2\sum_{k=1}^{T_p}|p(kT_s+nT+\xi)|^2}} \tag{2}$$

where T_s is the sampling period, T_p is the pulse duration, T is the separation of the pulses at the source and ξ is a correction to the pulse separation to compensate for source/receiver motion. This is effectively the normalised cross-correlation of two segments of the received signal. The indices *m* and *n* (approximately) select segments that correspond to identical waveforms when transmitted. Equation 2 measures the change to the originally

identical pulses as caused by the time-varying channel characteristics. The maximum operator in equation 2 is used to determine the change in pulse separation (ξ) between the two pulses at the receiver. Source and receiver motion could result in the pulse separation at the receiver being different from the pulse separation at the projector. Our intention here is to assume coherence loss is solely a function of delay, and we reduce the variation by averaging the result of equation 2 over multiple pulses. One limitation of this approach is that there is an implicit assumption that the coherence is constant over the bandwidth of the transmission. This is contrary to the finding that under certain assumptions and approximations (Yang 2010), the coherence time should obey

$$\tau_{1/e} \propto \frac{1}{f^{\alpha}\sqrt{R}} \tag{3}$$

where $\tau_{1/e}$ is the delay that causes the coherence to fall to $1/e$, f is frequency, R is range and α is a parameter that depends on environmental factors like water depth and sound speed profile. Theoretical studies have yielded values of $\alpha = 1$ (deep water) and $\alpha = 1.5$ (shallow water) but these studies depend on assumptions about the environment.Equation 2 does not account for the possibility of temporal coherence not being constant over the bandwidth of the pulse. We disregard this issue because we intend to use broadband pulses for CAS, so the coherence loss over a band is more pertinant than the loss at a particular frequency. The other limitation is that the coherence can only be measured at multiples of the separation of the transmitted pulses.

In a similar fashion to the definition of temporal coherence in equation 1, the spectral coherence can be defined as

$$\rho(f,\varsigma) = \frac{\langle P^*(f)P(f+\varsigma)\rangle}{\sqrt{\langle P^*(f)P(f)\rangle\langle p^*(f+\varsigma)p(f+\varsigma)\rangle}} \tag{4}$$

where $P(f) = \mathcal{F}\{p(t)\}$. In our analysis we found this formulation to be very sensitive to ambient noise and consequently we have avoided using it here.

If the received signal $r(n)$ is coherent for the entire length of a pulse then the optimum detector is

$$\delta(\tau) = \left|\sum_{n=0}^{N-1} s^*(n-\tau)r(n)\right| \tag{5}$$

where *s*(*n*) is the transmitted signal, This is known as the quadrature matched filter (McDonough and Whalen 1995). This test statistic is maximised if the phase between the transmitted signal and the received echo is constant over the integration period. This happens when the received signal experiences a constant delay propagating through the channel, i.e. the received echo has no coherence loss during the duty cycle. If there is coherence loss during the duty cycle, increasing *N* will not increase the matched filter output by as much as expected, and may even lead to a reduction (if the phase change goes beyond pi/2 the value will decrease). If the coherence loss is large then the test statistic

$$\delta(\tau) = \sum_{m=0}^{M-1}\left|\sum_{k=0}^{K-1} s^*(k+mK-\tau)r(k+mK)\right|^2 \tag{6}$$

is a better choice for detection. Ideally equation 6 is implemented with a matched filter of short duration segments (length K), such that the coherence within each segment is sufficient to provide a reasonable level of filtering gain. The final output is then obtained by incoherently integrating the segments. The advantage of this approach is that it is more robust under challenging conditions, when the coherence time of the acoustic channel is short. However, under more favourable conditions with longer coherence times, it will not perform as well as equation 5, because it is unable to take full advantage of the signal correlation over the entire duration of the pulse.

3 RESULTS

Three waveforms transmitted during the LCAS-16 trial were used to assess the coherence of the channel. The probe waveform, intended to probe the acoustic channel, is a chain of 128 linear frequency modulated (LFM) chirps, each 0.25 seconds long with a bandwidth of 1800 Hz and repeating every 0.25 seconds. This waveform was transmitted by a towed source and received by three fixed hydrophones. This waveform was used either at the start of the day or during a break in the trial, noting that the environmental conditions may not have corresponded to those during detection experiments. The CAS waveform, intended for target detection, was a 20 second duration LFM chirp with a bandwidth of 800 Hz. The PAS waveform, intended for target detection and as a benchmark to be compared to the CAS waveform, was a 1 second duration LFM chirp with an 800 Hz bandwidth repeated every 20 seconds. The CAS and PAS waveforms were transmitted (simultaneously in separate frequency bands) by the source vessel and remotely received on a second support vessel. The frequency evolution of the transmitted waveforms is illustrated in Figure 1. Coherence was determined for each of the two frequency bands using their respective PAS/CAS modulations, as well as for the combined frequency bands using both modulations.

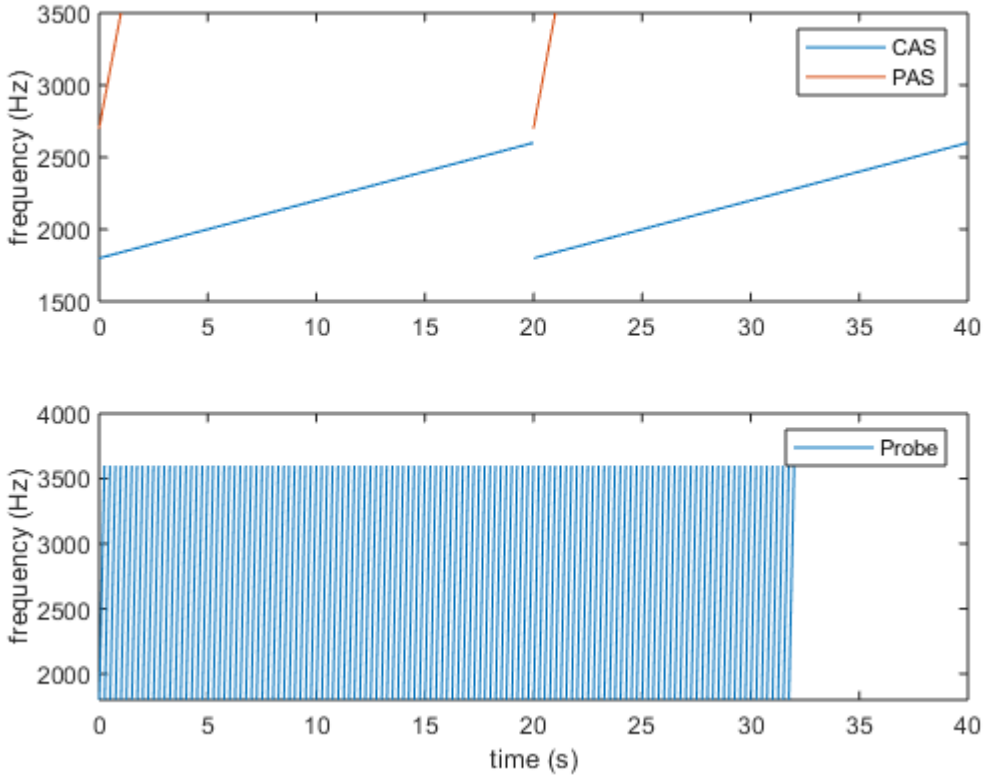

Figure 1: Waveforms used to estimate coherence

Section 3.2 discusses the dependence of detection upon coherent integration length (*K* from equation 6). Here, the PAS/CAS waveforms are transmitted from the source vessel, received and retransmitted by an echo repeater and then received on an array towed by the source vessel.

3.1 MEASURING COHERENCE DURING LCAS-16

Initially we consider measurements using the probe waveform (1800-3600Hz LFMs). In Figure 2 we compare the measurements of coherence for twelve blocks of transmissions. Each line represents a coherence measurement based on a single block of data, and all twelve were made using one hydrophone in the same geographical area over a 40 minute period. The figure shows the significant variability of the measurements and demonstrates the importance of averaging as much data as possible to achieve useful results. We believe this is a manifestation of the well-documented temporal and spatial variability of the underwater acoustic channel (Urick 1979).

During the LCAS-16 trial, the performance of CAS and PAS were to be compared by transmitting each at the same time in separate frequency bands. For this reason it is important to determine the difference in coherence of the two bands,1800-2600 Hz and 2700-3500 Hz. To approximate this situation the probe waveform data was divided into bands above and below 2650 Hz. Based on equation 3, we would expect to observe a lower coherence in the higher frequency band, and higher coherence in the lower frequency band. Figure 3 tends to confirm this expectation although the difference is small compared to the spread in the coherence measurements (c.f. Figure 2). This result was verified using the sign test (Lehmann 1986). It can be accepted with 90% confidence that higher frequencies show lower coherence.

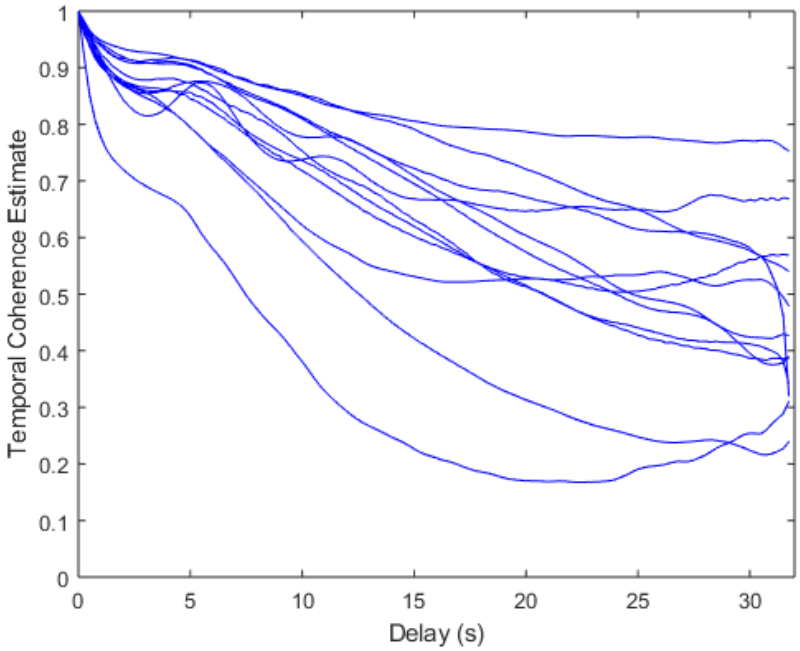

Figure 2: Coherence measurement for all twelve transmissions of the LFM sequence

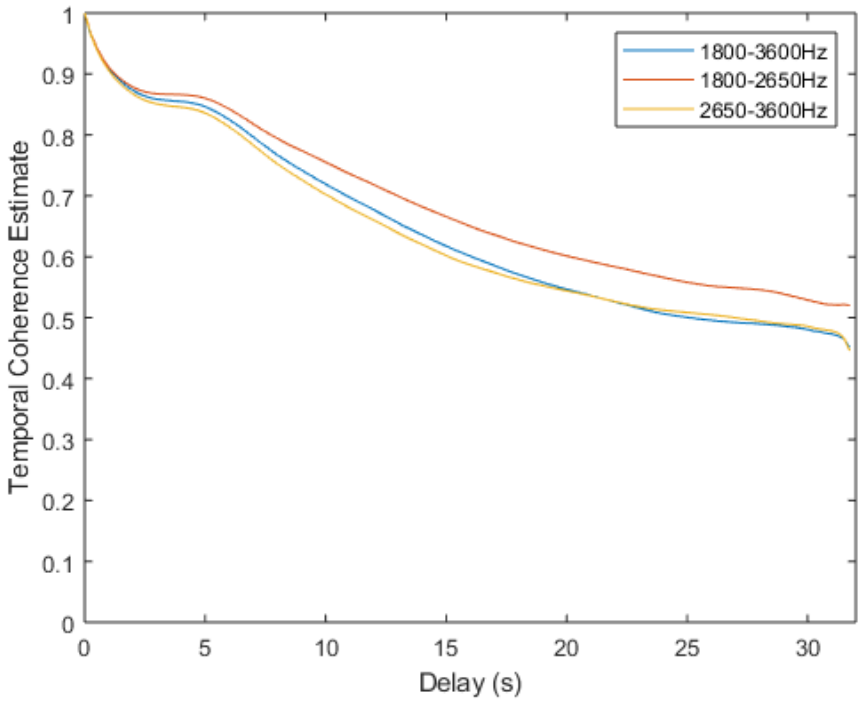

Figure 3: Coherence measurement using the full band and upper and lower parts of the LFM transmission

From equation 3 we would expect that the temporal coherence will decrease with increasing range, however, contrary to the theoretical prediction, Figure 4 shows that the hydrophone at the shortest range has the least coherence. Note that the derivation of equation 3 is based on a calculation for each of the modes in an assumed sound speed profile. The higher order modes (rays with the most reflections or bounces) are expected to show a lower coherence, but they are also expected to experience greater attenuation due to path loss. Coherence is impacted by sound speed profile, source/receiver motion and wave (internal and surface) spectra. We remain uncertain as to the true cause of this seemingly counterintuitive behaviour, demonstrating the need to improve our understanding of these factors. Since the measurement directly contradicts theory it is not surprising that the sign test (Lehmann 1986) indicates only a 20% confidence in the hypothesis that increased range leads to lower coherence.

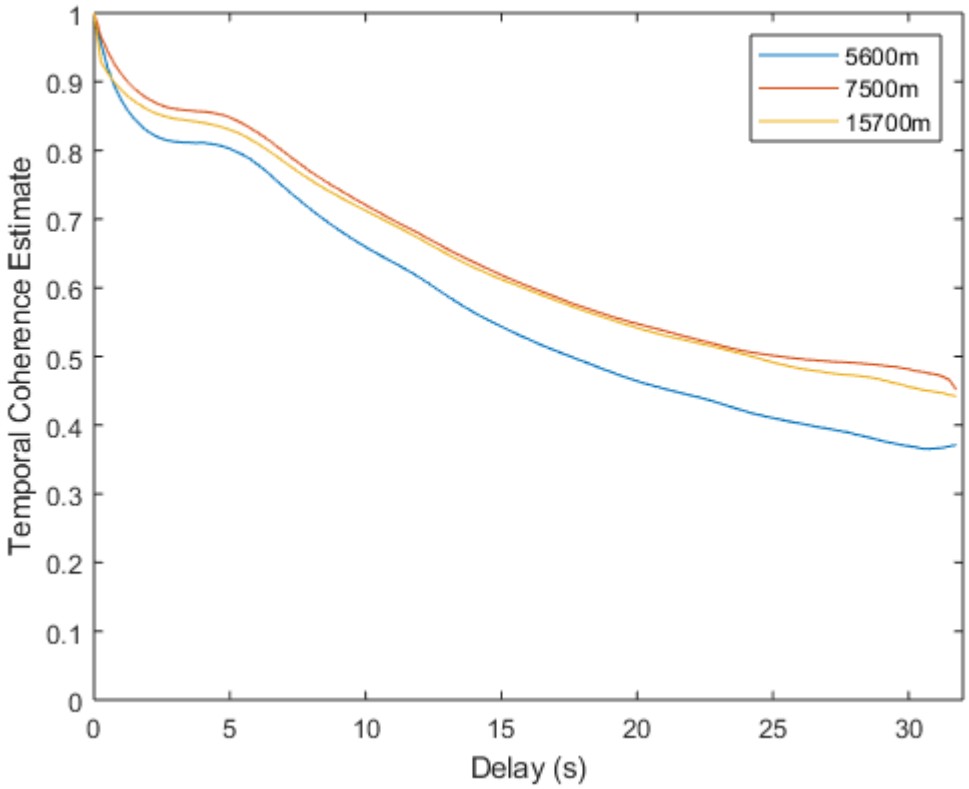

Figure 4: Temporal coherence estimate using LFM signals at different ranges

Loss of temporal coherence can be caused by changes in the properties of the acoustic channel over time. The most obvious change to the channel over time can be due to the waves and swell on the sea surface. Measurements presented here were taken on a single day when the sea state was very low. Coherence was also measured the previous day when the sea state and waves were more significant. The effect of higher sea state on decreasing coherence was diminished somewhat by operating below the surface duct (the duct was 30-40 metres and the array was deployed to 60 metres), thereby reducing interaction of the transmissions with the surface. However, the observations show that the sea state still had a significant impact on coherence. In Figure 5 the coherence measurement for the hydrophone and projector separated by 7000-8000 metres is shown for both sea states, and there is evidence that higher sea state (waves) has resulted in lower coherence.

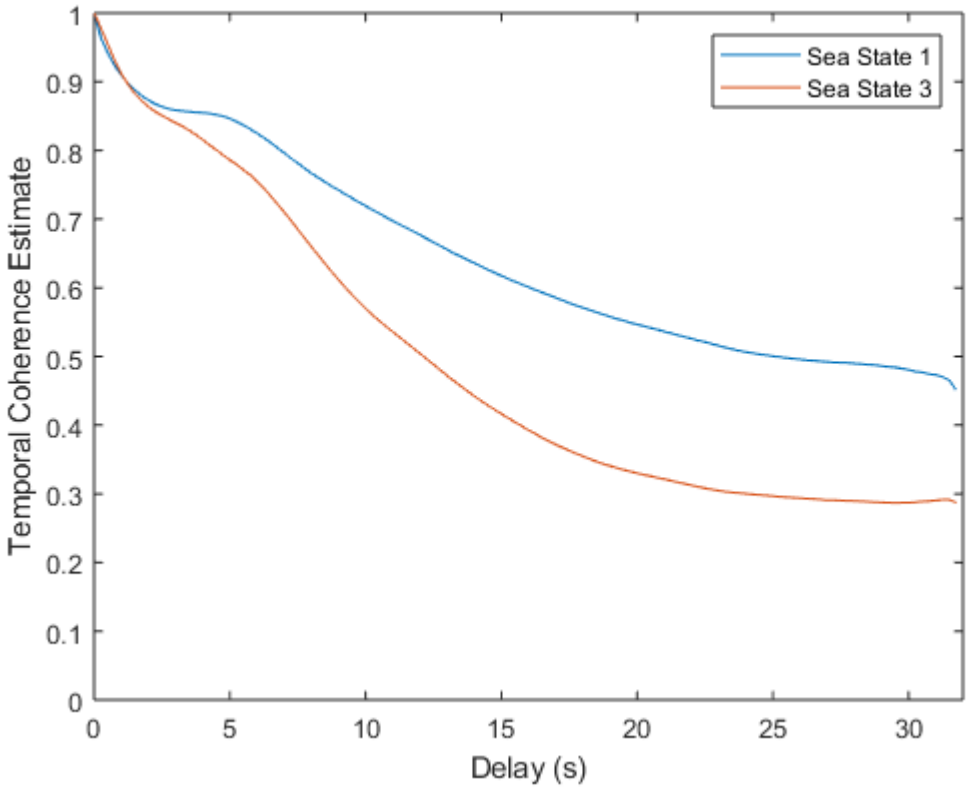

Figure 5: Temporal Coherence and sea roughness

The measurements of coherence considered so far have used a series of 0.25 second long LFM chirps repeated every 0.25 seconds so that temporal coherence could be estimated for delays that were multiples of a quarter of a second. We now consider using the CAS waveform described previously to measure coherence. We truncate the pulse at different pulse duration (vary the T_p from equation 2) to understand the dependence of the coherence estimates on this parameter. Unlike the former measurements the delays for which coherence could be measured were multiples of 20 seconds (the repeat rate of the transmission).

Figure 6 shows the results. Interestingly the curves in Figure 6 have a similar form to that observed by (Yang 2006) applying the same method to estimate coherence using LFM data. An obvious issue that was noted by Yang is that measurements of coherence are not available for delays less than the pulse repetition rate (20 seconds in this work and 50 seconds in the Yang paper).

It can be seen from Figure 6 that increasing the pulse duration used for the estimation results in lower coherence estimates. A possible explanation of this is that using longer LFM waveforms at the same sweep rate includes more high frequencies. Theory (equation 3) predicts and Figure 3 confirms that signals with higher frequency content have lower coherence.

A final note about Figure 6 is that at a delay of 20 seconds the coherence is still very high. This suggests that propagation conditions in the acoustic channel during the trial were quite benign. Integrating over the full 20 seconds of the transmission with pulses transmitted through this channel can be expected to give good detection performances.

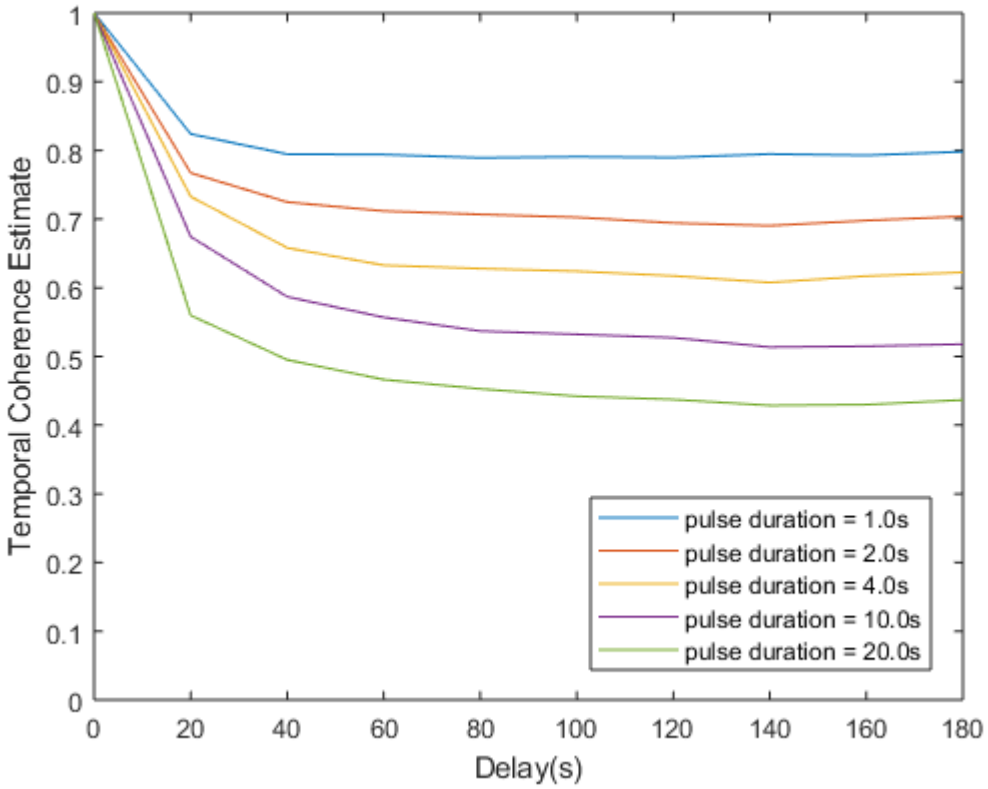

Figure 6: Coherence measurements during the detection phase of LCAS-16 experiments

3.2 DETECTION DURING LCAS-16

The receiver operating characteristic (ROC) curve of a detector plots probability of detection against the probability of false alarm. Detector performance is rated by its detection probability for a given false alarm rate. The ROC curve is theoretical, calculated from assumed statistics of the noise and target signals. In this work the background (noise) and target statistics are estimated by generating the probability density functions of these entities. The background estimation procedure excluded samples within 3 seconds of the start of a transmission, where high reverberation caused very high false alarm rates, and in beams within 36 degrees of endfire, where own ship noise and the projector caused high levels of noise and interference in the data. Failing to exclude this data from the estimation of the background resulted in such high false alarm rates that the detector would have been rendered useless. Normalisation using a cell averaging CFAR approach (Minkler and Minkler J. 1990) was also applied to the test statistic of equation 6.

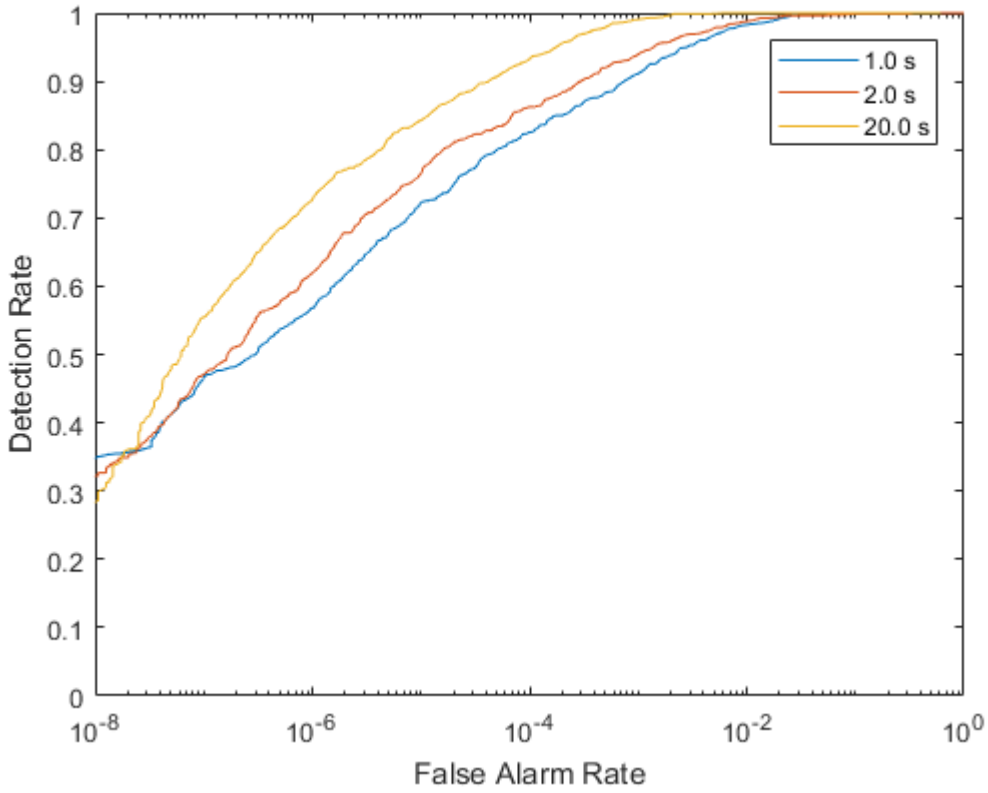

Figure 7: Receiver operating characteristic for different integration lengths during the LCAS-16 trial

The results of the ROC curve analysis are shown in Figure 7. The results suggest that for this trial the longer the integration lengths offered better detection performance. This is the expected result as a longer integration time increases the gain of the signal (due to the action of the strong law of large numbers) relative to noise. Coherence loss does not seem to have significantly limited this behaviour possibly due to the low sea state during the trial and the comparatively robust behaviour of the LFM pulse (Colin and Beerens 2011) in low coherence conditions. This is consistent with our measurements above indicating that the coherence loss of the channel during the trial was very low.

4 CONCLUSIONS AND FUTURE WORK

In this paper we report the results of measurements of temporal coherence derived from data collected during the LCAS-16 trial. Our analyses suggest that temporal coherence decreases when the signal centre frequency is increased and when seas are rough. We also expected the coherence to decrease with range, and while this was supported by some measurements, we encountered other measurements that contradicted this expectation. We also observed that the temporal coherence was highly variable. Highly variable channel properties is a common observation when measuring the acoustic channel often resulting in the received signal level being highly variable..

The objective of the work was to determine the ideal coherent integration period for a CAS sonar detector. In view of this goal we havepresented results on the effect of coherent integration length has on detection performance. The result was that for the benign environmental conditions of the trial and the robust propagation behaviour of the LFM chirp the longest coherent integration length tested gave the best detection performance.

The future goal of this work is to determine the optimal integration length for a CAS sonar detector, based on a knowledge of the prevailing conditions, such as the acoustic environment, operating frequency, sea state and target range. During the more recent LCAS-18 trial, further coherence measurements were made. It is envisaged that the ongoing analysis of this data will provide further insight to the ideal integration length. Selection of

the integration length will depend on defining an acceptable trade-off between false alarms and detection success for the system involved.

In future, we plan to conduct coherence measurements where more rigorous efforts are made to maintain constant range between source and receiver. The use of an array rather than a single hydrophone as the receiver would also be desirable, as this would allow the averaging of multiple element measurements.

5 Acknowledgment

This work was made possible by the LCAS Multi-National Joint Research Project (MN-JRP) including as Participants the NATO Centre for Maritime Research and Experimentation, the Defence Science and Technology Organisation (AUS), the Department of National Defence of Canada Defence Research and Development Canada (CAN), the Defence Science and Technology Laboratory (UK), Centro di Supporto e Sperimentazione Navale-Italian Navy (ITA) the Norwegian Defence Research Establishment (NOR), the Defence Technology Agency (NZL), and the Office of Naval Research (USA).

6 References

Baggenstoss, Paul M. 1994. “On Detecting Linear Frequency-Modulated Waveforms in Time and Frequency Dispersive Channels: Alternatives to Segmented Replica Correlation.” *IEEE Journal of Oceanic Engineering* 19 (4): 591-598.

Colin, Mathieu, and S. Peter Beerens. 2011. “False-Alarm Reduction for Low-Frequency Active Sonar with BPSK Pulses: Experimental Results.” *Journal of Oceanic Engineering* 52-59.

Lehmann, Erich L. 1986. *Testing Statistical Hypotheses.* 2nd. New York: Springer-Verlag.

McDonough, Robert N., and Anthony D. Whalen. 1995. *Detection of Signals in Noise.* San Diego: Academic Press.

Minkler, G., and Minkler J. 1990. *CFAR.* Baltimore: Magellan.

Plate, Randall, and Doug Grimmett. 2015. “High Duty Cycle (HDC) Sonar Processing Interval and Bandwidth Effects for the TREX' 13 Dataset.” *MTS/IEEE Oceans' 15.* Genova, Italy.

Plate, Randall, and Doug Grimmett. 2016. “Temporal and Doppler Coherence Limits for the Underwater Acoustic Channel during the LCAS' 15 High Duty Cycle Sonar Experiment.” *MTS/IEEE Oceans 2016.* Monterey.

Urick, Robert J. 1979. *Sound Propagation in the Sea.* Ann Arbor: University of Michigan Library.

van Walree, Paul A. 2013. “Propagation and Scattering Effects in Underwater Acoustic Communication Channels.” *IEEE Journal of Oceanic Engineering* 38 (4): 614-631.

Yang, T. C. 2006. “Measurements of temporal coherence of sound transmissions through shallow water.” *Journal of the Acoustical Society of America* 120 (5): 2595-2614.

Yang, T. C.. 2010. “Temporal Coherence of Normal Modes in an Ocean Waveguide.” *Second International Shallow-Water Acoustics Conference.* Shanghai.

Zhang, ZhongShan, Keping Long, Athanasios V. Vasilakos, and Lajos Hanzo. 2016. “Full-Duplex Wireless Communications: Chalenges, Solutions, and Future Directions.” *Proceedings of the IEEE* 104 (7): 1369-1409.